

TWO DIMENSIONAL PATTERNS IN A MODEL FOR THE ELECTROHYDRODYNAMIC INSTABILITY OF NEMATIC LIQUID CRYSTALS

P. DE BROUWER and D. WALGRAEF†

*Service de Chimie-Physique,
Université Libre de Bruxelles,
Bd du Triomphe, CP 231,
B-1050, Brussels, Belgium.*

ABSTRACT. The study of the different patterns which appear beyond the electrohydrodynamic instability of nematic liquid crystals is performed in the framework of a dynamical model of the Proctor-Sivashinsky type. This model describes the experimentally observed transitions between rolls, zig-zag and bimodal structures.

1. Introduction

In the recent years, there has been much interest for pattern forming instabilities in nematic liquid crystals, both experimentally [1-2] and theoretically [3-6]. It is now well known that a thin layer of nematic liquid crystal, submitted to an oscillating electrical field of increasing amplitude, presents a sequence of transitions between different types of structures ending in complex spatio-temporal regimes [1-5]. Usually, the following structures are successively observed : straight rolls, undulated rolls, oblique or zig-zag rolls, bimodal structures and finally states of high spatio-temporal complexity.

The theoretical description of these structures and of the electrohydrodynamic convection in general is extremely difficult, due to the complexity of the underlying nemato-electrohydrodynamics, and the time dependence of the external forcing. It has however been possible to perform the linear stability analysis of the homogeneous steady state and to compute the threshold for pattern formation, the

† Director of Research, National Fund for Scientific Research (Belgium).

neutral surface and the linear growth rate of the unstable modes [5], but a systematic derivation of the nonlinear terms of the corresponding amplitude equations from the underlying dynamics is not available yet. Amplitude equations, based on symmetry arguments, have nevertheless been derived for each type of structure and they satisfactorily describe various aspects of electrically driven liquid crystals. Despite their interest, these equations are not able to describe the transitions between the different structures, nor their relative stability. Hence it would be interesting to rely on a reduced dynamical model which encompasses the various instability thresholds and plays here the role of the Swift-Hohenberg equation for Rayleigh-Bénard convection [7].

It is why we propose to describe the behavior of nematic liquid crystals near the electrohydrodynamic instability with a reduced dynamical model for an order parameterlike variable which takes into account a minimal set of basic elements, namely the intrinsic anisotropy of the system, which is known to affect the selection and stability of spatial patterns [8], and the gradient dependence of the nonlinear couplings. This model reproduces the sequence of observed patterns but also suggests that bimodal structures should be stable in a closed domain of the parameter space. The fact that the boundary of this domain corresponds to a phase instability is consistent with the observed defect mediated disordered states that appear for increasing field intensities.

2. The model

Following the linear stability analysis and the near threshold description performed by Bodenschatz et al. for electrohydrodynamic convection in nematics [5], the linear growth rate of the order parameterlike variable may be written, near the instability threshold, as

$$- \{ \epsilon [\partial_x^2 + s \partial_y^2] + [1 + \partial_x^2 + \partial_y^2]^2 + 2\eta \partial_x^2 \partial_y^2 + \tau \partial_y^4 \} \quad (1)$$

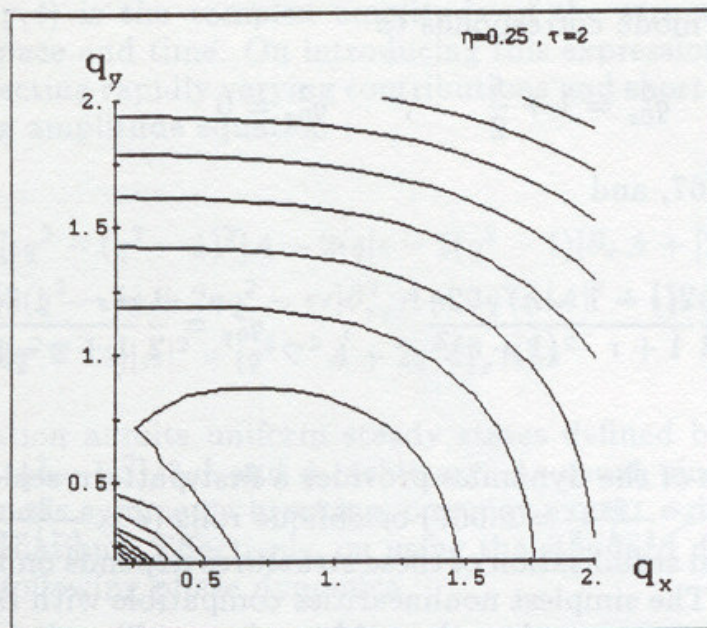
or

$$\{ \epsilon [q_x^2 + s q_y^2] - [1 - q_x^2 - q_y^2]^2 - 2\eta q_x^2 q_y^2 - \tau q_y^4 \} \quad (2)$$

in Fourier space. ϵ is the reduced distance to threshold $(V^2 - V_c^2)/V_c^2$ where V is the amplitude of the applied voltage and V_c its threshold value. s , η and τ are positive materials parameters reflecting the anisotropy of the system, and the critical wavenumber has been scaled to one. The x axis being the easy axis, s is larger than one, and, in the following, we will consider $s = 2$, $\eta = 0.25$ and $\tau = 1.5$, values that are consistent with the analysis of Bodenschatz et al. [5]

The corresponding marginal stability surface is thus given by (fig.1)

$$\epsilon = \frac{[1 - q_x^2 - q_y^2]^2 + 2\eta q_x^2 q_y^2 + \tau q_y^4}{q_x^2 + s q_y^2}, \quad (3)$$



Contour plot of the marginal stability surface for the anisotropic PS model

Marginal stability curve of the anisotropic PS model

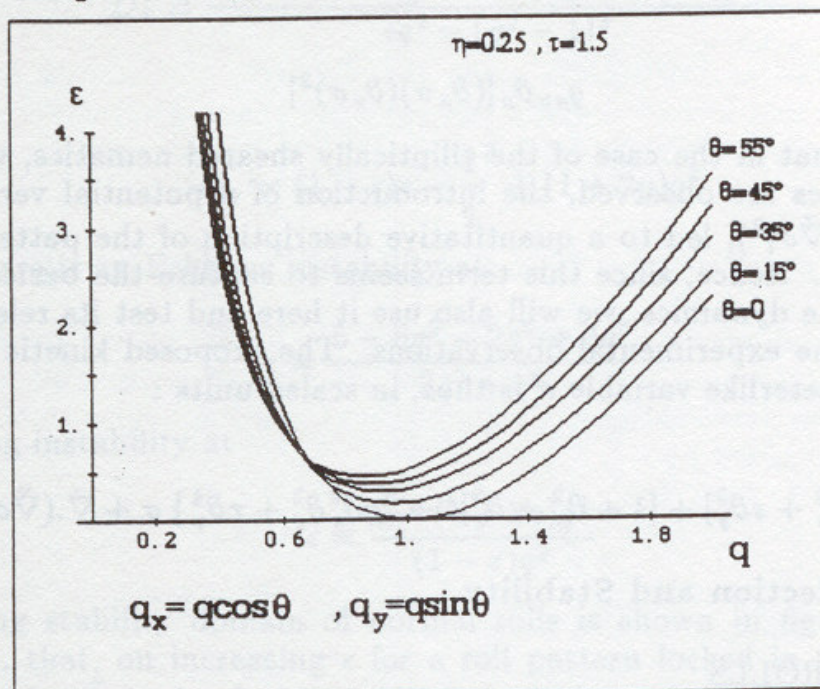


Figure 1 : Contour plot of the marginal stability surface and marginal stability curve for different wavevector orientations in the case of the linear growth rate given in (1).

and the fastest growing mode corresponds to

$$q_{0x}^2 = 1 + \frac{\epsilon}{2}, \quad q_{0y}^2 = 0 \quad (4)$$

for $0 < \epsilon < \frac{2\eta}{s-1-\eta} = 0.667$, and

$$q_{0x}^2 = 1 + \frac{\epsilon}{2} - (1+\eta) \frac{1}{2} \frac{\epsilon(s-1-\eta) - 2\eta}{1+\tau - (1+\eta)^2}, \quad q_{0y}^2 = \frac{1}{2} \frac{\epsilon(s-1-\eta) - 2\eta}{1+\tau - (1+\eta)^2} \quad (5)$$

for $\epsilon > \frac{2\eta}{s-1-\eta} = 0.667$

Hence, the linear part of the dynamics provides a first pattern selection mechanism towards normal ($\epsilon < \frac{2\eta}{s-1-\eta} = 0.667$) or oblique rolls ($\epsilon > \frac{2\eta}{s-1-\eta} = 0.667$).

Of course, the eventual stabilisation of these structures depends on the nonlinear terms of the dynamics. The simplest nonlinearities compatible with the amplitude equations derived in [5] correspond to the cubic scalar nonlinearity of the Swift-Hohenberg equation, σ^3 , where σ is the order parameterlike variable. However, this term is not able to stabilize bimodal structures [9] and one has to introduce gradient dependent nonlinearities. On performing a systematic expansion in the gradients, the first nonlinear terms able to stabilize bimodal structure are of the form

$$g_{\mu\nu} \partial_\mu [(\partial_\nu \sigma)(\partial_\nu \sigma)^2] \quad (6)$$

Let us note that in the case of the elliptically sheared nematics, where similar pattern sequences are observed, the introduction of a potential version of these terms, $g \vec{\nabla} \cdot (\vec{\nabla} \sigma |\vec{\nabla} \sigma|^2)$, led to a quantitative description of the pattern formation phenomena [10]. Hence, since this term seems to capture the basics of the nonlinear part of the dynamics, we will also use it here and test its relevance to the description of the experimental observations. The proposed kinetic equation for the order parameterlike variable σ is thus, in scaled units :

$$\partial_t \sigma = - \{ \epsilon [\partial_x^2 + s \partial_y^2] + [1 + \partial_x^2 + \partial_y^2]^2 + 2\eta \partial_x^2 \partial_y^2 + \tau \partial_y^4 \} \sigma + \vec{\nabla} \cdot (\vec{\nabla} \sigma |\vec{\nabla} \sigma|^2) \quad (7)$$

3. Pattern Selection and Stability

3.1. NORMAL ROLLS

Since the first structure to bifurcate from the electrohydrodynamic instability corresponds to normal rolls (i.e. with wavevector parallel to the easy axis 0x), let us derive their amplitude equation and study their stability. The normal rolls are defined by :

$$\sigma(x, y, t) = A(x, y, t) e^{iqx} + \bar{A}(x, y, t) e^{-iqx} \quad (8)$$

where $A(x, y, t)$ is the complex amplitude of the structure and may be slowly varying in space and time. On introducing this expression in the kinetic equation (7) and neglecting rapidly varying contributions and short scale effects, one obtains the following amplitude equation :

$$\begin{aligned} \partial_t A = & [\epsilon q^2 - (q^2 - 1)^2] A - 2iq[\epsilon - 2(q^2 - 1)] \partial_x A + [2(3q^2 - 1) - \epsilon] \partial_{xx}^2 A \\ & + [2(q^2 - 1) + 2\eta q^2 - \epsilon s] \partial_{yy}^2 A - 3q^4 A |A|^2 + [12iq^3 \partial_x A + 4q^2 \partial_{xx}^2 A \\ & + 2q^2 \nabla^2 A] |A|^2 - [q^2 \nabla^2 \bar{A} + 2q^2 \partial_{xx}^2 \bar{A}] A^2 \end{aligned} \quad (9)$$

This equation admits uniform steady states defined by $A_0 = R_0 \exp i\phi_0$, with $R_0^2 = [\epsilon q^2 - (q^2 - 1)^2]/3q^4$ and ϕ_0 arbitrary. As usual, since these patterns appear via a continuous symmetry breaking, one may expect a diffusive behavior of their phase perturbations. Effectively, on using the standard derivation procedure, one obtains the following phase dynamics :

$$\partial_t \phi = D_x \partial_{xx}^2 \phi + D_y \partial_{yy}^2 \phi \quad (10)$$

where

$$D_x = \frac{\epsilon(q^4 + 3) - (q^2 - 1)^2(3q^2 + 4 + 5q^{-2})}{\epsilon q^2 - (q^2 - 1)^2} \quad (11)$$

and

$$D_y = (1 - s)\epsilon - \frac{1}{q^2} + (1 + 2\eta)q^2 \quad (12)$$

Hence, there is an Eckhaus instability at

$$\epsilon = \frac{5 - 6q^2 - 2q^6 + 3q^8}{3q^2 + q^6} \quad (13)$$

and a zig-zag instability at

$$\epsilon = \frac{1 - (1 + 2\eta)q^4}{(1 - s)q^2} \quad (14)$$

The resulting stability domain of normal rolls is shown in figure 2. It shows, for example, that, on increasing ϵ for a roll pattern locked in the first unstable wavevector ($\vec{q} = \vec{1}_x$), the first instability occurs at $\epsilon = 0.5$ and is of the zig-zag type, while for normal rolls with the optimal wavevector, the first instability occurs at $\epsilon = 1.68$ and is of the Eckhaus type. In any case, since the phase stability limits of normal rolls form a closed domain, this pattern always becomes unstable on increasing ϵ .

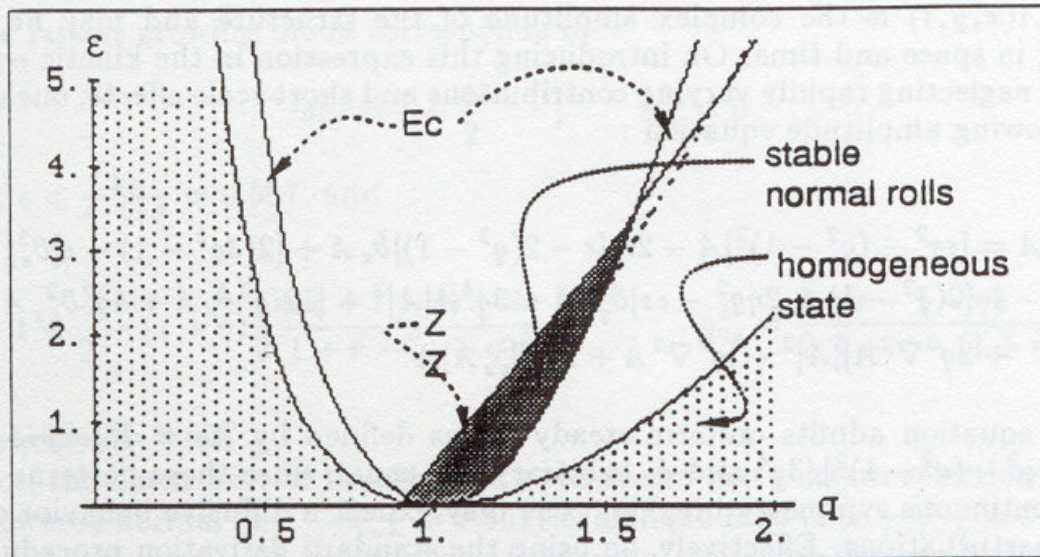


Figure 2 : Stability diagram for normal roll solutions of the amplitude equations (9).

3.2. UNDULATED ROLLS

Near a phase diffusive instability, since the diffusion coefficients become small or even negative, one has to include higher order space derivatives in the phase dynamics. For the normal rolls described in the preceding section, one obtains :

$$\partial_t \phi = D_x \partial_{xx}^2 \phi + D_y \partial_{yy}^2 \phi - \partial_{xxx}^4 \phi - 2(1 + \eta) \partial_{xxyy}^4 \phi - (1 + \tau) \partial_{yyyy}^4 \phi \quad (15)$$

One sees on the diagram displayed in figure 2 that the phase instability that a roll pattern encounters on increasing ϵ is of the zig-zag type. Hence the system will develop phase perturbations of wavevectors k perpendicular to the x axis and of linear evolution given by :

$$\partial_t \phi_k = -[D_y k^2 + (1 + \tau) k^4] \phi_k \quad (16)$$

and, for $D_y < 0$, there exists a whole band of unstable wavevectors k , the most unstable corresponding to

$$k_0 = \sqrt{-\frac{D_y}{2(1+\tau)}} \quad (17)$$

In the immediate neighbourhood of the instability, the system will thus develop transient undulated rolls which are intermediate states between the normal rolls and the new bifurcating structure corresponding to oblique rolls.

3.3. OBLIQUE ROLLS

Above the zig-zag instability of normal rolls, one expects structures with non vanishing y components of their wavevectors. Since unstable modes with wavevectors $q_1 = q_x \vec{1}_x + q_y \vec{1}_y$ and $q_2 = q_x \vec{1}_x - q_y \vec{1}_y$ ($q_1^2 = q_2^2$) have the same linear growth rate, the order parameterlike variable may be written as :

$$\begin{aligned} \sigma(x, y, t) = & A(x, y, t)e^{i(q_x x + q_y y)} + \bar{A}(x, y, t)e^{-i(q_x x + q_y y)} \\ & + B(x, y, t)e^{i(q_x x - q_y y)} + \bar{B}(x, y, t)e^{-i(q_x x - q_y y)} \end{aligned} \quad (18)$$

The corresponding amplitude equations are given by :

$$\begin{aligned} \partial_t A = & [\epsilon(q_x^2 + s q_y^2) - (q^2 - 1)^2 - 2\eta q_x^2 q_y^2 - \tau q_y^4] A \\ & - 2i q_x [\epsilon + 2 - 2q_x^2 - 2(1 + \eta)q_y^2] \partial_x A \\ & - 2i q_y [\epsilon s + 2 - 2(1 + \eta)q_x^2 - 2(1 + \tau)q_y^2] \partial_y A \\ & + [4q_x^2 + 2(q^2 - 1) + 2\eta q_y^2 - \epsilon] \partial_{xx}^2 A + 8(1 + \eta) q_x q_y \partial_{xy}^2 A \\ & + [4q_y^2 + 2(q^2 - 1) + 2\eta q_x^2 + 6\tau q_y^2 - \epsilon s] \partial_{yy}^2 A \\ & - 3q_1^4 |A|^2 A - 2[q_1^2 q_2^2 + 2(\vec{q}_1 \cdot \vec{q}_2)^2] |B|^2 A - [q_1^2 \nabla^2 \bar{A} + 2\vec{q}_1 \cdot \vec{\nabla}(\vec{q}_1 \cdot \vec{\nabla} \bar{A})] A^2 \\ & + [12i q_1^2 (\vec{q}_1 \cdot \vec{\nabla} A + 4\vec{\nabla}(\vec{q}_1 \cdot \vec{\nabla} A) + 2q_1^2 \nabla^2 A) |A|^2 \\ & + 2[q_2^2 \nabla^2 A + 2i q_2^2 (\vec{q}_1 \cdot \vec{\nabla} A) + 2(2i \vec{q}_1 \cdot \vec{q}_2 + \vec{q}_2 \cdot \vec{\nabla})(\vec{q}_2 \cdot \vec{\nabla} A)] |B|^2 \\ & + 2[i(q_1^2 + 2\vec{q}_1 \cdot \vec{q}_2)(\vec{q}_1 + \vec{q}_2) \cdot \vec{\nabla} B + 2\vec{q}_1 \cdot \vec{\nabla}(\vec{q}_2 \cdot \vec{\nabla} B) + (\vec{q}_1 \cdot \vec{q}_2) \nabla^2 B] A \bar{B} \\ & + 2[i(q_1^2 + 2\vec{q}_1 \cdot \vec{q}_2)(\vec{q}_1 - \vec{q}_2) \cdot \vec{\nabla} \bar{B} - 2\vec{q}_1 \cdot \vec{\nabla}(\vec{q}_2 \cdot \vec{\nabla} \bar{B}) - (\vec{q}_1 \cdot \vec{q}_2) \nabla^2 \bar{B}] A \bar{B} \end{aligned} \quad (19a)$$

$$\begin{aligned}
\partial_t B = & [\epsilon(q_x^2 + sq_y^2) - (q^2 - 1)^2 - 2\eta q_x^2 q_y^2 - \tau q_y^4] B \\
& - 2iq_x [\epsilon + 2 - 2q_x^2 - 2(1 + \eta)q_y^2] \partial_x B \\
& + 2iq_y [\epsilon s + 2 - 2(1 + \eta)q_x^2 - 2(1 + \tau)q_y^2] \partial_y B \\
& + [4q_x^2 + 2(q^2 - 1) + 2\eta q_y^2 - \epsilon] \partial_{xx}^2 B - 8(1 + \eta)q_x q_y \partial_{xy}^2 B \\
& + [4q_y^2 + 2(q^2 - 1) + 2\eta q_x^2 + 6\tau q_y^2 - \epsilon s] \partial_{yy}^2 B \\
& - 3q_2^4 |B|^2 B - 2[q_1^2 q_2^2 + 2(\vec{q}_1 \vec{q}_2)^2] |A|^2 B - [q_2^2 \nabla^2 \bar{B} + 2\vec{q}_2 \cdot \vec{\nabla} (\vec{q}_2 \cdot \vec{\nabla} \bar{B})] B^2 \\
& + [12iq_2^2 (\vec{q}_2 \cdot \vec{\nabla} B + 4\vec{\nabla} (\vec{q}_2 \cdot \vec{\nabla} B) + 2q_2^2 \nabla^2 B) |B|^2 \\
& + 2[q_2^2 \nabla^2 B + 2iq_2^2 (\vec{q}_1 \cdot \vec{\nabla} B) + 2(2i\vec{q}_1 \cdot \vec{q}_2 + \vec{q}_2 \cdot \vec{\nabla}) (\vec{q}_2 \cdot \vec{\nabla} B)] |A|^2 \\
& + 2[i(q_1^2 + 2\vec{q}_1 \cdot \vec{q}_2) (\vec{q}_1 + \vec{q}_2) \cdot \vec{\nabla} A + 2\vec{q}_1 \cdot \vec{\nabla} (\vec{q}_2 \cdot \vec{\nabla} A) + (\vec{q}_1 \cdot \vec{q}_2) \nabla^2 A] B \bar{A} \\
& + 2[i(q_1^2 + 2\vec{q}_1 \cdot \vec{q}_2) (\vec{q}_1 - \vec{q}_2) \cdot \vec{\nabla} \bar{A} - 2\vec{q}_1 \cdot \vec{\nabla} (\vec{q}_2 \cdot \vec{\nabla} \bar{A}) - (\vec{q}_1 \cdot \vec{q}_2) \nabla^2 \bar{A}] A B
\end{aligned} \tag{19b}$$

These equations admit stationary solutions corresponding to patterns of uniform amplitudes which may be of

- the oblique roll type :

$$A = R_0 \exp i \phi_0, \quad B = 0, \quad \text{or} \quad B = R_0 \exp i \phi_0, \quad A = 0$$

with

$$R_0^2 = \frac{\epsilon(q_x^2 + sq_y^2) - (q_1^2 - 1)^2 - 2\eta q_x^2 q_y^2 - \tau q_y^4}{3q_1^4}, \quad \phi_0 = \text{cst} \tag{20}$$

- the bimodal type :

$$A = S_0 \exp i \phi_0, \quad B = S_0 \exp i \psi_0$$

with

$$S_0^2 = \frac{\epsilon(q_x^2 + sq_y^2) - (q_1^2 - 1)^2 - 2\eta q_x^2 q_y^2 - \tau q_y^4}{3q_1^4 + 2[q_1^2 q_2^2 + 2(\vec{q}_1 \vec{q}_2)^2]}, \quad \phi_0, \psi_0 = \text{cst} \tag{21}$$

The oblique rolls are stable for $3q_1^4 < 2[q_1^2 q_2^2 + 2(\vec{q}_1 \vec{q}_2)^2]$ or $\cos^2 \theta > 1/4$, θ being the angle between the wavevectors q_1 and q_2 . Bimodal structures are stable for $3q_1^4 > 2[q_1^2 q_2^2 + 2(\vec{q}_1 \vec{q}_2)^2]$ or $\cos^2 \theta < 1/4$. Hence, since q_y has a tendency to increase and q_x to decrease for increasing ϵ (cf. eq. (5)), we expect first the formation of zig-zag structures corresponding to alternate domains of oblique rolls of wavevectors q_1 and q_2 . The phase dynamics and stability domains of these structures may be determined as usual [11]. However, when the angle between q_1 and q_2 exceeds $\pi/3$, a transition to bimodal structures should occur.

3.4. BIMODAL STRUCTURES

As seen in the preceeding section, uniform bimodal structures are stable when their underlying wavevectors q_1 and q_2 make an angle θ such that $\pi/3 < \theta < 2\pi/3$. Since this angle increases with ϵ , the expected final structure corresponds to squares built on orthogonal wavevectors symmetric versus the easy axis $0x$. The phase dynamics of this pattern may be derived along the usual lines [11], and one finds :

$$\begin{aligned}\partial_t \phi &= D_{XX}^1 \partial_{XX}^2 \phi + D_{XY}^1 \partial_{XY}^2 \phi + D_{YY}^1 \partial_{YY}^2 \phi \\ &\quad + D_{XX}^2 \partial_{XX}^2 \psi + D_{XY}^2 \partial_{XY}^2 \psi + D_{YY}^2 \partial_{YY}^2 \psi \\ \partial_t \psi &= D_{YY}^1 \partial_{XX}^2 \psi + D_{XY}^1 \partial_{XY}^2 \psi + D_{XX}^1 \partial_{YY}^2 \phi \\ &\quad + D_{YY}^2 \partial_{XX}^2 \phi + D_{XY}^2 \partial_{XY}^2 \phi + D_{XX}^2 \partial_{YY}^2 \phi\end{aligned}\quad (22)$$

where $X = (x + y)/\sqrt{2}$ and $Y = (x - y)/\sqrt{2}$. The diffusion coefficients are analytical functions of the various parameters of the dynamics and have been explicitly computed [11]. It turns out that the square pattern is only stable in a closed domain as shown in figure 3.

Hence, the square patterns are destabilized via a phase instability which induces the spontaneous nucleation of topological defect. As a result, they should naturally experience the experimentally observed defect mediated disorganization [12]. Furthermore, non variational contributions to the dynamics, which have been omitted in the present description, should strongly influence defect motion and take care of some aspects of the spatio-temporal complexity observed in this system [13]

4. Conclusions

We showed that the pattern formation phenomena that occur in the electrohydrodynamic instability of nematics can be described qualitatively with a reduced dynamical which takes essentially into account the intrinsic anisotropy of the system and the gradient dependence of the nonlinear couplings. This model provides an alternative to the too complex nematohydrodynamics for the study of the generic properties of pattern formation in anisotropic systems. The sequence of patterns, going from rolls to bimodal structures, results from the competition between linear anisotropy effects and the structure of the nonlinear couplings. Furthermore, it appears that the latter are responsible of the fact that bimodal structures are only stable in a closed domain of the parameter space. This is consistent with the defect mediated disorganization of the system which is observed for increasing field intensity. Of course, a quantitative description of these phenomena requires the numerical analysis of the model, the fitting of some of its parameters, and eventually the introduction of non variational effects. We nevertheless think that the understanding of pattern formation in liquid crystal instabilities could benefit much from this description and that the proposed model could play here the same role that the Swift-Hohenberg equation played for Rayleigh-Bénard convection.

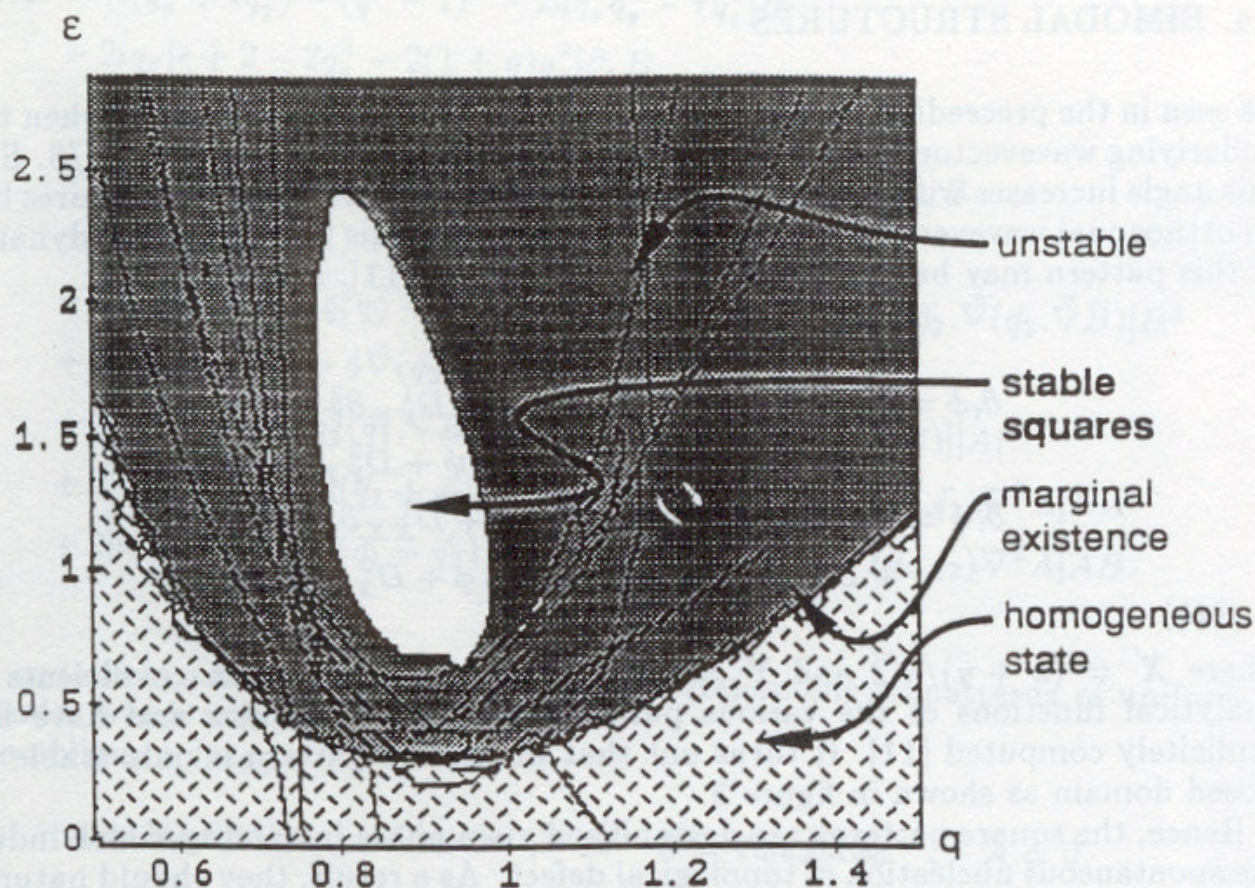


Figure 3 : Stability diagram for square patterns solutions of the amplitude equations (9) for $s = 2$, $\eta = 0.25$ and $\tau = 1.5$.

Acknowledgments. D.W. is grateful to the Fundacion Andes (Chile) for its support during the realization of this work.

References

1. A.Joets and R.Ribotta, *J.Physique* **47** (1986), p. 595.
2. S.Kai and W.Zimmerman, *Prog.Theor Phys.* **99** (1989), p. 458.
3. E.Dubois-Violette, P.G.De Gennes and O.Parodi, *J.Physique* **32** (1971), p. 305.
4. W.Pesch and L.Kramer, *Z.Physik B* **63** (1986), p. 121.
5. E.Bodenschatz, W.Zimmerman and L.Kramer, *J.Physique* **49** (1988), p. 1875.
6. D.Walgraef, in "Nematics," J.M.Coron et al., eds., Kluwer, Dordrecht, 1991, p. 391.
7. J.Swift and P.C.Hohenberg, *Phys.Rev. A* **15** (1977), p. 319.
8. D.Walgraef and C.Schiller, *Physica D* **27** (1987), p. 423.
9. D.Walgraef, *Solid state Phenomena* **3-4** (1988), p. 77.

10. E. Guazzelli, G. Dewel, P. Borckmans and D. Walgraef, *Physica D* **35** (1989), p. 220.
11. P. De Brouwer, "Pattern Formation in Nematics subjected to an Oscillating Electrical Field," Licentiaat Thesis, Vrije Universiteit Brussel, 1991.
12. J. Toner and D. Nelson, *Phys. Rev. B* **23** (1981), p. 316.
13. D. Walgraef, *Pattern Evolution in Extended Nonequilibrium Systems*, preprint, Free University of Brussels, 1992.

A. De Wit*, P. Borckmans, G. Dewel
 Service de Chimie Physique and
 Centre for Nonlinear Phenomena and Complex Systems
 Université Libre de Bruxelles, CP 231
 1050 Bruxelles
 Belgium

ABSTRACT. To understand recent experimental observations of localized Turing structures in the presence of periodic oscillations, the pattern formation in two and three dimensional homogeneous model reaction-diffusion systems is fully discussed. The influence of several types of inputs on the selected and the selected Turing structure is then numerically studied.

1. Introduction

Recent experimental results [1, 2] have strongly induced a renewal of interest in the study of pattern formation in nonequilibrium systems [3]. This spontaneous spatial self-organization in chemistry, proposed theoretically by Turing in 1952 [4], had never been observed experimentally until the conception about ten years of new kinds of reaction. These occur in a thin piece of gel (or differently along two opposite walls) by controlled reservoirs containing the reactants at the chemical-kinetic anisotropic concentration. The gel supports the reaction-diffusion effects while preserving all diffusion processes. The work has showed a new observation of Turing structure: stationary periodic patterns of concentration in space that arise from the coupling of diffusion and nonlinear chemical reactions.

After that finding in the class of dissipative structures arising from interactions between reaction, diffusion and transport phenomena for open chemical systems [5], the observed structures are two or three dimensional (2D, 3D) according to the importance of the pattern generated by the forcing. These results give questions about the influence of several of parameters on the selection and the organization of patterns.

In this paper, we study numerically the problem in 2D and 3D. We first review in Section 2 the reaction in systems with homogeneous forcing of reactants. Section 3 studies the effect of several types of inputs on 2D pattern formation. We study the behavior of 3D tapered patterns in Section 4.

2. Homogeneous forcing of reactants

We study the pattern selection problem in chemistry on a two-Species reaction-diffusion model. The equations [6] whose equations of evolution take the form

* A.S.R.-I, (Belgium) Fellow.

† Under Research Assistant with the F.N.R.S. (Belgium).